Realization of regular arrays of nanoscale resistive switching blocks in thin films of Nb-doped $SrTiO_3$

Ruth Muenstermann, Regina Dittmann, Krzysztof Szot, Shaobo Mi, Chun-Lin Jia, Paul Meuffels, and Rainer Waser

Citation: Appl. Phys. Lett. **93**, 023110 (2008);
View online: https://doi.org/10.1063/1.2959074
View Table of Contents: http://aip.scitation.org/toc/apl/93/2
Published by the American Institute of Physics

Realization of regular arrays of nanoscale resistive switching blocks in thin films of Nb-doped $SrTiO_3$

Ruth Muenstermann,[a] Regina Dittmann,[b] Krzysztof Szot,[c] Shaobo Mi,[d] Chun-Lin Jia,[e] Paul Meuffels,[f] and Rainer Waser[g]
Institute of Solid State Research, Forschungszentrum Juelich, 52425 Juelich, Germany

(Received 15 April 2008; accepted 22 June 2008; published online 16 July 2008)

We report on the realization of short-range-ordered arrays of nanoscale resistive switching blocks in epitaxial Nb-doped $SrTiO_3$ thin films. These blocks can be individually addressed by the tip of a conductive tip atomic force microscope and reversibly switched between a high and a low resistance state reaching an R_{off} to R_{on} ratio of up to 50. Scanning micrometer-scale areas with an appropriately biased tip, all blocks within the scanned area can be switched between the two resistive states. We suggest a connection between these nanoscale switching blocks and defect-rich nanoclusters which were detected with high resolution transmission electron microscopy. © *2008 American Institute of Physics*. [DOI: 10.1063/1.2959074]

Searching for future concepts of nonvolatile resistive memory devices, an upsurge of interest in thin perovskite films as resistive switching layers has arisen ever since the discovery of an electric field induced resistance change in manganites and titanates as well as zirconates.[1–3] The switching of these materials is highly local in both lateral and vertical direction.[4–8] This restriction of the switching process to the region directly below the interface favors the use of thin films whereas the lateral inhomogeneity could be advantageous in terms of future scalability. For undoped $SrTiO_3$, it was shown that the switching occurs along crystalline defects which extend through the sample and form a network of nanometer-sized filamentary conduction paths.[4,9] This makes $SrTiO_3$ a very promising candidate for a nonvolatile memory in the terabit regime. Since the distribution of switchable filaments in undoped $SrTiO_3$ is however very irregular, the application of this material in future resistive random access memory crucially depends on the development of thin film fabrication routes which guarantee a more uniform arrangement of these filaments. Doping $SrTiO_3$ with transition metals improves the stability of the resistive switching and may be a tool to influence the extension and the local distribution of switching units in $SrTiO_3$ thin films.[2] In this work, donor-doped $SrTi_{1-x}Nb_xO_3$ thin films are therefore investigated with a conductive tip atomic force microscope (LC-AFM). We explore the local current distribution and the arrangement of intrinsic nanoscale switching units of these films and relate it to the microstructure determined by high resolution transmission electron microscopy (HR-TEM).

Thin films were prepared by pulsed laser deposition employing a KrF excimer laser ($\lambda=248$ nm) with an energy density of 5 J/cm^2 at a frequency of 10 Hz. A $SrTiO_3$ target with a Nb concentration of 1 wt % and commercially available $SrTiO_3(001)$ or $NdGaO_3(110)$ substrates were used. We chose a substrate temperature of 700 °C and an oxygen partial pressure of approximately 10^{-6} mbar. Such low oxygen partial pressures are necessary in order to grow well-conducting Nb-doped $SrTiO_3$ films.[10,11] In addition argon was let into the chamber resulting in an overall pressure of 10^{-4} mbar during deposition. X-ray diffraction measurements prove that all films are grown epitaxially and *c*-axis oriented. The thickness of was estimated to be 250 nm. The electronic structure of the films was investigated by x-ray photoemission spectroscopy (XPS). While the Ti2*p* coreline exhibits two spin-orbit doublets resulting from Ti(IV) (major part) and Ti(III) (minor part), only one spin-orbit doublet can be safely determined for the Nb3*d* coreline. Nb is therefore completely ionized and the classical electronic compensation of donor-doped $SrTiO_3$ takes place.[12] An identical behavior was found in Nb-doped TiO_2.[13] Although the overall conductivity of the samples is semiconducting, XPS spectra of the bandgap region show a small metallic peak at the upper edge of the bandgap indicating localized metallic states. In order to investigate the local nature of the conductivity and the switching behavior of the samples, we performed LC-AFM measurements of all films. All measurements were carried out with a Jeol JSPM 4210 microscope employing a PtIr-coated AFM tip. The chamber containing the sample was evacuated to a background pressure of 10^{-5} mbar in order to reduce the influence of surface adsorbates. The current compliance was set to 1 μA since higher currents cause a delamination of the PtIr coating. The lateral electrical resolution of the tip was demonstrated to be in the order of a few nanometers which is consistent with theoretical estimations of the effective contact area between tip and sample.[4,9,14] Finite element simulations show that the main part of a voltage applied between tip and sample drops directly below the tip.[15] Any tip induced resistive switching therefore takes place within the surface near region of the sample. Since no changes of the surface structure during or after the scanning with the biased tip were visible, a decomposition of the film in connection with the external voltage and an adsorbed water film as it is described by Pellegrino *et al.* did not take place in our case.[16]

The LC-AFM topography image and the corresponding local current distribution of a 1 wt % Nb doped $SrTiO_3$ film grown on $NdGaO_3(110)$ are shown in Fig. 1. The images were recorded with a negatively biased tip ($V_{tip}=-3$ V). The

[a]Author to whom correspondence should be addressed. Tel.: +49-2461-615339. Electronic mail: ru.muenstermann@fz-juelich.de.
[b]Tel.: +49-2461-61 4760. Electronic mail: r.dittmann@fz-juelich.de.
[c]Tel.: +49-2461-61 6479. Electronic mail: k.szot@fz-juelich.de.
[d]Tel.: +49-2461-61 2413. Electronic mail: s.mi@fz-juelich.de.
[e]Tel.: +49-2461-61 2408. Electronic mail: c.jia@fz-juelich.de.
[f]Tel.: +49-2461-61 4223. Electronic mail: p.meuffels@fz-juelich.de.
[g]Tel.: +49-2461-61 5811. Electronic mail: r.waser@fz-juelich.de.

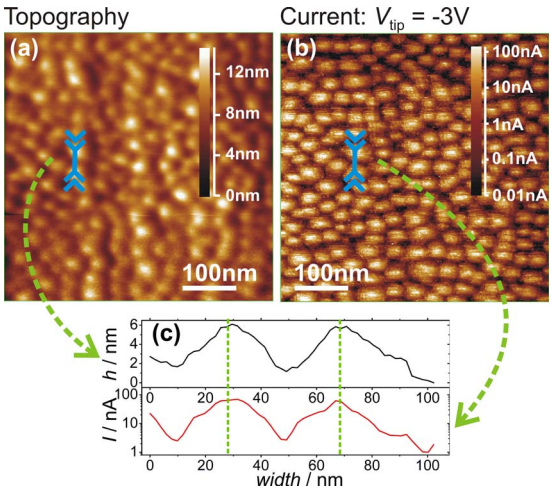

FIG. 1. (Color online) Parts (a) and (b) show LC-AFM images of a Nb-doped $SrTiO_3$ film grown under low oxygen pressure. The surface of the film consists of protrusions with a conductive centre and practically nonconductive boundaries [part (c)] forming an array of conductive spots.

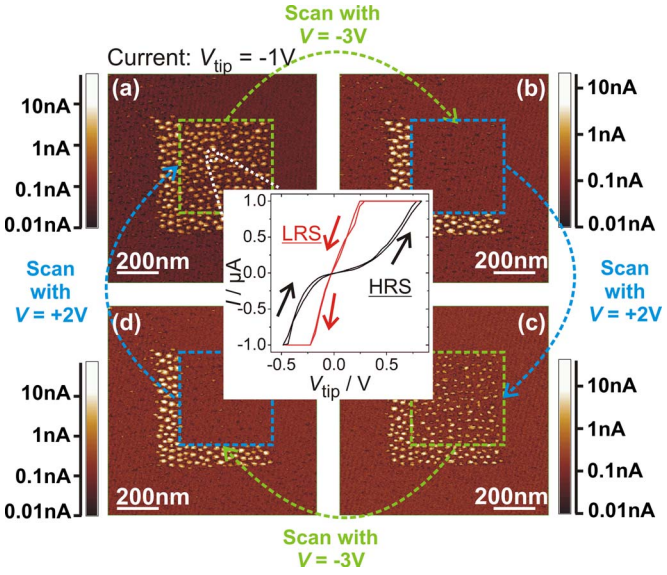

FIG. 2. (Color online) Reversible resistive switching in Nb-doped $SrTiO_3$. The current images show an array of conducting spots which can be switched between two different resistance states. The current compliance is instrumentally limited to 1 μA.

surface is covered with little protrusions [Fig. 1(a)], which possess a width between 30 and 50 nm and a height between 1 and 4 nm. The root mean square roughness of the surface is approximately 1 nm. Since the topography and the local current distribution are identical for films grown on $NdGaO_3(110)$ and $SrTiO_3$ (001) substrates, respectively (not shown here), we conclude that the observed protrusions are not caused by the accommodation of substrate-induced misfit strain. The local current distribution [Fig. 1(b)] shows circular spots, which exhibit a width of approximately 30 nm and correspond directly to the protrusions on the topography. The center of each protrusion is conductive, while the boundaries are almost nonconductive. This correlation between the current distribution and the topographic structure can be seen clearly by comparison of two linescans which are drawn at the same place in the topography and the current image, respectively [Fig. 1(c)]. The possibility that the variation of the local conductivity is a tip induced measurement artifact (for example, caused by a limited electrical or topographical resolution of the tip) can be ruled out for two reasons. On the one hand, the lateral electrical resolution of the tip is in the order of a few nanometers and is thereby noticeably smaller than the observed feature sizes.[4,9,14] On the other hand, we have observed samples (which were grown under different deposition conditions and are not presented in this article) which had similar surface features as the sample shown in Fig. 1 but showed a very different conductivity pattern. If there was any tip induced measurement artifact connected to the LC-AFM measurement, it should however produce the same effect for all measured samples. We thereby conclude that there is no such artifact and that the correlation seen in Fig. 1 is indeed a property inherent to the sample.

While nanometer-sized inhomogeneities in the conductivity of perovskites have been observed before and even a similar trend in the correlation between topography and local conductivity has been found in some samples, those conductivity patterns are still very irregular.[6,17] In our case however the protrusions form an almost well ordered array of conducting spots with diameters of approximately 30 nm [Fig. 1(b)]. The conductivity and surface pattern depend critically on the deposition conditions. Films that were deposited at a higher temperature (800 °C) grew in layer-by-layer mode and showed a much smoother surface and a less pronounced conductivity pattern. The lower substrate temperature during the growth of the film shown in Fig. 1 resulted in a transition from layer-by-layer to three-dimensional growth and in the formation of the protrusions and conducting spots observed by LC-AFM. This influence of the deposition conditions on the film growth combined with the correlation between topography and conductivity pattern opens up the possibility of systematic future engineering of the conductivity pattern.

By applying an external voltage between the tip and the sample, it is possible to change the resistance of every conducting spot individually. The central part of Fig. 2 shows an *I-V* curve of a typical single conducting spot (indicated by the white dashed circle), which was recorded by placing the AFM tip over the spot and varying the applied voltage. The *I-V* curve has a clear hysteresis and shows a bipolar switching behavior. A sufficiently high negative tip voltage switches the spot into a high resistance state (HRS), while a positive tip voltage switches the spot into a low resistance state (LRS). An R_{off} to R_{on} ratio of up to 50 can be obtained. Stable switching curves can be recorded as long as the tip has not drifted away from the conducting spot. The switching behavior can be reproduced for a large amount of conducting spots by scanning the positively ($V_{tip} \geqslant 2$ V) or negatively ($V_{tip} \leqslant -3$ V) biased tip over a defined area of the sample. All four current distribution images in the outer parts of Fig. 2 are recorded with a tip voltage of −1 V. While in Fig. 2(a), all spots inside the inner square are conductive, a scan over the area of the green dashed square with a negative tip voltage of at least −3 V switches all spots inside the scan area "off" [Fig. 2(b)]. A subsequent scan with a positive tip voltage of at least +2 V recovers the conductivity of the previously switched off spots [Fig. 2(c)], while yet another scan with −3 V switches them off again [Fig. 2(d)]. The tip voltage of −1 V can be regarded as a readout voltage and does not change the conductivity. The difference in write voltages between the *I-V* measurement and the lateral scans (around ± 0.5 and +2/−3 V, respectively) is due to the different time that the tip resides above each spot to be switched. In sum-

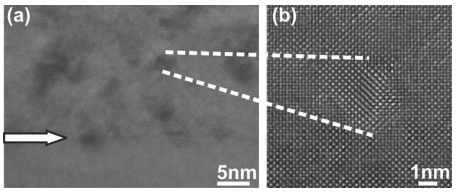

FIG. 3. HR-TEM investigations reveal defect-rich clusters embedded in the matrix of the film. (a) shows a low magnification out-of-plane lattice image with several clusters, while (b) shows a higher magnification of a single cluster. Lattice defects and lattice distortion are detectable in both out-of-plane and plan-view images.

mary, it is possible to switch each of the 30 nm wide spots individually between two different resistance states. This switching can however only be observed if the measurement is carried out under vacuum conditions (as described above). Samples that were measured in air showed a similar conductivity pattern but the increased amount of surface adsorbates made measurements very difficult. Switching could not be found in those measurements. The observed switching polarities (a negative voltage at the tip switches the scanned area into a high resistance state, a positive voltage switches it into a low resistance state) are consistent with the current image in Fig. 1(b), which was recorded with a negative tip voltage of −3 V while switching the scanned area off. The scan with the switching voltage of −3 V itself still shows the high conductivity of the LRS state, while any following scan shows the almost nonconductive surface of the HRS state.

In order to gain insight into the microstructure of the film and thus the structural nature of the protrusions or the conducting spots, HR-TEM measurements of a Nb-doped $SrTiO_3$ film grown under low oxygen pressure on a $SrTiO_3(100)$ substrate have been performed. They show that the film is grown coherently on the substrate without any misfit dislocations at the interface. Neither grain boundaries nor growth island boundaries are found. In both plan-view, and cross-sectional view, defect-rich clusters with a density of 10^{18} cm^{-3} and dimensions between 2 and 20 nm are observed (Fig. 3). Lattice defects and lattice distortion are detectable. Figure 3(a) includes an interface between the $SrTiO_3$ substrate and the film as marked by an arrow. The clusters can be seen as areas with a dark contrast in the image. They appear in the film as well as at the interface. A similar density and distribution of defects is found in all areas of the film including the surface area. The observed defect clusters may result from the bombardment with high energetic particles under low oxygen pressure during the film growth.[18] At the given growth temperature and the high repetition rate of 10 Hz, those clusters could not heal up.

Summarizing the TEM and LC-AFM results for our films, we see a high density of lattice-distorted, defect-rich nanoclusters which have diameters in the range from 2 to 20 nm. Since the nucleation tendency and growth velocity during the film growth are strongly dependent on the defect structure and vary for defect-rich and defect-free areas, the specific defect structure of the films results in a laterally inhomogeneous growth process. A two-dimensional layer-by-layer growth is prohibited and a three-dimensional growth takes place resulting in the observed protrusions at the surface of the sample. Moreover, the LC-AFM results indicate an inhomogeneous conductivity distribution on the sample surface, which according to our XPS results can be attributed to an inhomogeneous distribution of Ti^{3+}. Since the conducting blocks are situated at the center of the protrusions, it is possible that these centers correspond to defect-rich areas which appear as elevated hills due to an enhanced nucleation tendency during film growth and which may act as a place of a redox reaction from Ti^{3+} to Ti^{4+} during the tip-induced switching process. We could prove the possibility of such a reaction with XPS by scanning the sample with a biased tip and monitoring the Ti^{3+}/Ti^{4+} ration. While in undoped $SrTiO_3$, grown in a layer-by-layer growth mode, resistive switching occurs by a voltage induced oxygen vacancy movement along one-dimensional extended filaments, the switching in Nb-doped $SrTiO_3$ grown in a three-dimensional growth mode could be confined to a different kind of defect structure.[4,9] The redox reaction takes place within the surface-near region of this structure while the sample acts as a sink or source of oxygen. The exact nature of the switching mechanism itself remains however unclear. Although a redox process as suggested above seems reasonable, other effects that are related to the surface and possible space charge layers need to be considered as well.[19] Overall more experimental evidence is necessary to either confirm or disprove these assumptions.

In summary, we have demonstrated for Nb-doped $SrTiO_3$ that by appropriate choice of the deposition conditions, we succeeded in fabricating arrays of 30 nm wide resistive switching blocks, which can be switched between LRS and HRS by applying an external voltage. We attribute these resistive switching blocks to the specific defect structure of our thin films.

We thank Tobias Menke for helpful discussions and the critical reading of the manuscript. This work was financially supported by Intel Inc., Santa Clara.

[1] A. Asamitsu, Y. Tomioka, H. Kuwahara, and Y. Tokura, Nature (London) **388**, 50 (1997).
[2] A. Beck, J. G. Bednorz, Ch. Gerber, C. Rossel, and D. Widmer, Appl. Phys. Lett. **77**, 139 (2000).
[3] Y. Watanabe, J. G. Bednorz, A. Bietsch, Ch. Gerber, D. Widmer, A. Beck, and S. J. Wind, Appl. Phys. Lett. **78**, 3738 (2001).
[4] K. Szot, W. Speier, G. Bihlmayer, and R. Waser, Nat. Mater. **5**, 312 (2006).
[5] C. Rossel, G. I. Meijer, D. Brémaud, and D. Widmer, J. Appl. Phys. **90**, 2892 (2001).
[6] X. Chen, N. J. Wu, J. Strozier, and A. Ignatiev, Appl. Phys. Lett. **89**, 063507 (2006).
[7] M. J. Rozenberg, I. H. Inoue, and M. J. Sánchez, Phys. Rev. Lett. **92**, 178302 (2004).
[8] A. Sawa, T. Fujii, M. Kawasaki, and Y. Tokura, Appl. Phys. Lett. **88**, 232112 (2006).
[9] K. Szot, R. Dittmann, W. Speier, and R. Waser, Phys. Status Solidi (RRL) **1**, 86 (2007).
[10] T. Tomio, H. Miki, H. Tabata, T. Kawai, and S. Kawai, J. Appl. Phys. **76**, 5886 (1994).
[11] A. Leitner, C. T. Rogers, J. C. Price, D. A. Rudman, and D. R. Herman, Appl. Phys. Lett. **72**, 3065 (1998).
[12] R. Moos, A. Gnudi, and K. Härdtl, J. Appl. Phys. **78**, 5042 (1995).
[13] D. Morris, Y. Dou, J. Rebane, C. E. J. Mitchell, R. G. Egdell, D. S. L. Law, A. Vittadini, and M. Casarin, Phys. Rev. B **61**, 13445 (2000).
[14] W. Frammelsberger, G. Benstetter, J. Kiely, and R. Stamp, Appl. Surf. Sci. **253**, 3615 (2007).
[15] J. Fleig and J. Maier, Solid State Ionics **86**, 1351 (1996).
[16] L. Pellegrino, E. Bellingeri, A. S. Siri, and D. Marré, Appl. Phys. Lett. **87**, 064102 (2005).
[17] H. B. Moon, C. H. Kim, J. S. Ahn, and J. H. Cho, J. Phys. Chem. B **110**, 24277 (2006).
[18] P. R. Willmott and J. R. Huber, Rev. Mod. Phys. **72**, 315 (2000).
[19] R. Meyer and R. Waser, Sens. Actuators B **101**, 335 (2004).